Neuropharmacology 113 (2017) 467–479

Contents lists available at ScienceDirect

Neuropharmacology

journal homepage: www.elsevier.com/locate/neuropharm

# Agmatine ameliorates type 2 diabetes induced-Alzheimer's disease-like alterations in high-fat diet-fed mice via reactivation of blunted insulin signalling

Somang Kang [a, b], Chul-Hoon Kim [c], Hosung Jung [a, b], Eosu Kim [d], Ho-Taek Song [e], Jong Eun Lee [a, b, *]

[a] Department of Anatomy, Yonsei University College of Medicine, Seoul, 120-752, South Korea
[b] BK21 Plus Project for Medical Sciences, and Brain Research Institute, Yonsei University College of Medicine, Seoul, 120-752, South Korea
[c] Department of Pharmacology, Yonsei University College of Medicine, Seoul, 120-752, South Korea
[d] Department of Psychiatry, Yonsei University College of Medicine, Seoul, 120-752, South Korea
[e] Department of Diagnostic Radiology, Yonsei University College of Medicine, Seoul, 120-752, South Korea

ARTICLE INFO

*Article history:*
Received 10 May 2016
Received in revised form
18 October 2016
Accepted 28 October 2016
Available online 31 October 2016

*Keywords:*
High-fat diet
Brain insulin resistance
Agmatine
Alzheimer's disease

ABSTRACT

The risk of Alzheimer's disease (AD) is higher in patients with type 2 diabetes mellitus (T2DM). Previous studies in high-fat diet-induced AD animal models have shown that brain insulin resistance in these animals leads to the accumulation of amyloid beta (Aβ) and the reduction in GSK-3β phosphorylation, which promotes tau phosphorylation to cause AD. No therapeutic treatments that target AD in T2DM patients have yet been discovered. Agmatine, a primary amine derived from L-arginine, has exhibited anti-diabetic effects in diabetic animals. The aim of this study was to investigate the ability of agmatine to treat AD induced by brain insulin resistance. ICR mice were fed a 60% high-fat diet for 12 weeks and received one injection of streptozotocin (100 mg/kg/ip) 4 weeks into the diet. After the 12-week diet, the mice were treated with agmatine (100 mg/kg/ip) for 2 weeks. Behaviour tests were conducted prior to sacrifice. Brain expression levels of the insulin signal molecules p-IRS-1, *p*-Akt, and *p*-GSK-3β and the accumulation of Aβ and p-tau were evaluated. Agmatine administration rescued the reduction in insulin signalling, which in turn reduced the accumulation of Aβ and p-tau in the brain. Furthermore, agmatine treatment also reduced cognitive decline. Agmatine attenuated the occurrence of AD in T2DM mice via the activation of the blunted insulin signal.



## 1. Introduction

Clinical and epidemiological studies indicate a higher risk of Alzheimer's disease (AD) among patients with type 2 diabetes mellitus (T2DM) (Craft and Watson, 2004). Previous studies have found a high-fat diet to be common risk factor for T2DM and AD (Edwards et al., 2011; Valls-Pedret and Ros, 2013; Willette et al., 2015). Based on this work, rodents models with various diet-induced AD-like alterations have been established to examine the pathogenesis of AD in T2DM (Arnold et al., 2014; Luo et al., 1998; McNeilly et al., 2011; Stranahan et al., 2008). Using these models, several studies have demonstrated that brain insulin resistance is likely to be the main cause of AD-like alterations (Haan, 2006; Jayaraman and Pike, 2014; Kim and Feldman, 2012; Ma et al., 2015). Insulin signalling is important for various neuronal functions (Belfiore et al., 2009), and may be involved in the regulation of synaptic activities, cognitive processes (Zhao and Alkon, 2001), and learning and memory (Kim and Feldman, 2015). Furthermore, insulin stimulates Aβ extracellular secretion to inhibit its intracellular accumulation (de la Monte, 2012; Gasparini et al., 2001; Pratico et al., 2001; Watson et al., 2003) and blocks GSK-3β via phosphorylation to inhibit neuronal tau phosphorylation (Balaraman et al., 2006; Clodfelder-Miller et al., 2005; Schubert et al., 2004; Takashima, 2006). Therefore, AD may develop when insulin is unable to work in the brain due to brain insulin resistance (Kim and Feldman, 2012).

An adequate therapeutic treatment that targets AD in T2DM patients has not yet been established. Although metformin, which

* Corresponding author. Department of Anatomy, Yonsei University College of Medicine, Seoul, 120-752, South Korea.
*E-mail address:* jelee@yuhs.ac (J.E. Lee).

http://dx.doi.org/10.1016/j.neuropharm.2016.10.029

is a popular treatment for T2DM, has been applied to AD, its effects remain controversial (Gupta et al., 2011; McNeilly et al., 2012; Moore et al., 2013; Picone et al., 2015). Meanwhile, we believe that agmatine could be a therapeutic option for treating AD in individuals with T2DM. Altered arginine metabolism is associated with diabetes (Lee et al., 2011) as well as the deterioration of memory functions, similar to those found in AD patients (Liu et al., 2014). Arginine is metabolized into several bioactive molecules, including agmatine. Agmatine, an endogenous aminoguanidine compound made from arginine by arginine decarboxylase, has had positive effects in animal models of several diseases, such as diabetes, stroke, spinal cord injury, and cognitive decline (Ahn et al., 2014; Cui et al., 2012; Park et al., 2013; Song et al., 2014; Su et al., 2009). For example, agmatine has exhibited anti-diabetic effects in type 1 and type 2 diabetic animals (Chang et al., 2010; Hwang et al., 2005; Ko et al., 2008; Su et al., 2009). Several studies have demonstrated the pharmacological potential of agmatine in treating cognitive decline and memory impairment in various animal models (Arteni et al., 2002; Liu and Bergin, 2009; McKay et al., 2002; Moosavi et al., 2014; Rastegar et al., 2011; Zarifkar et al., 2010). Recently, agmatine has been shown to improve memory function in type 1 diabetes-induced memory decline (Bhutada et al., 2012). Also, our previous report revealed that agmatine activates insulin signal transductions in the brain to prevent cognitive decline induced by an intracerebroventricular streptozotocin injection (Song et al., 2014).

Although the effects of agmatine on diabetes and memory impairment have been independently reported, the possible therapeutic effect of agmatine on AD-like alterations in T2DM mice characterized by brain insulin resistance has not yet been investigated. The aim of the present study was to show that the regulation of insulin signalling by agmatine attenuates AD-like alterations in T2DM mice characterized by brain insulin resistance.

## 2. Materials and methods

### 2.1. Materials

Agmatine, streptozotocin, and glucose were purchased from Sigma Aldrich (St. Louis, MO, USA). Antibodies against IRS-1, p-IRS-1 (Tyr 632), p-tau (Ser 202, Tyr 205), TNF-α, and IL-1β were purchased from Santa Cruz Biotechnology (Dallas, TX, USA). Antibodies for detecting Akt, amyloid beta, and horseradish peroxidase (HRP)-conjugated anti-mouse, anti-rabbit, and anti-goat IgG antibodies were purchased from Abcam (Cambridge, UK). Beta-actin, FITC, or rhodamine-conjugated donkey anti-rabbit or anti-mouse antibodies and 4′,6-diamidino-2-phenylindole (DAPI) were purchased from Millipore (Billerica, MA, USA). Other antibodies against *p*-Akt (Ser473), *p*-GSK-3β (Ser9), and GSK-3β were purchased from Cell Signalling Technology (Beverly, MA, USA). The polyvinylidene difluoride (PVDF) membrane for western blot assay was purchased from Millipore. The chemiluminescence reagents (ECL) for western blot assay were from Life Technologies (Carlsbad, CA, USA). The high-fat diet (60% kcal fat) was purchased from Research Diets (New Brunswick, NJ, USA) and normal diet was purchased from LabDiet (St. Louis, MO, USA). The portable glucometer (CareSensII Meter) was purchased from Pharmaco (NZ) Ltd. (Auckland, New Zealand). The serum insulin ELISA was purchased from ALPCO (Windham, NH, USA) and tissue insulin ELISA was purchased from Shibayagi (Gumma, Japan). The amyloid beta ELISA is purchased from Invitrogen (Carlsbad, CA, USA). All the other chemicals used in this experiment were purchased from Sigma Aldrich.

### 2.2. Establishment of the T2DM mice with AD-like alterations characterized by brain insulin resistance

Adult male ICR mice (7 weeks old, Central Lab Animal Inc., Seoul, Korea) were used in this study. The mice were raised in a standard laboratory animal facility under a 12 h light/dark cycle and had free access to food and water *ad libitum*. All procedures were conducted in accordance with the Yonsei University College of Medicine Animal Care and Use Committee and the National Institutes of Health guidelines for the Care and Use of Laboratory Animals. We modified previously established methods (Byrne et al., 2015; Jiang et al., 2012; Luo et al., 1998; Rahigude et al., 2012; Tahara et al., 2011)to develop a T2DM mouse model with AD-like alterations characterized by brain insulin resistance. After a week of acclimatization to the laboratory conditions, mice were randomly divided into two groups. Mice were administered either a normal chow diet (NC; 13.1% kcal fat) or a high-fat diet (HFD; 60% kcal fat) for 12 weeks (Table 1). The mice fed HFD were injected once at week 4 with a low dose of streptozotocin [STZ; 100 mg/kg/ip, dissolved in citrate buffer (pH 4.4)] to shorten the time taken for the animal model to be established by inducing partial insulin deficiency (Fig. 1).

Mice with fasting serum glucose level >200 mg/dl, body weight >55 g, and impaired glucose, insulin tolerance were classified as T2DM (Tabak et al., 2012). T2DM mice were divided into two groups: HFD mice treated with saline and HFD mice treated with agmatine (HFD + AGM; 100 mg/kg/ip, dissolved in saline). These groups were treated with agmatine daily for 2 weeks (Fig. 1). Twelve mice were included in each group (a total of 36 mice were used).

### 2.3. Determination of body weight and serum glucose levels

Body weights (BW) and fasting serum glucose levels (Piletz et al., 2013) of all animals were monitored weekly. To measure fasting glucose levels, mice were fasted for 4 h before the test. Blood glucose concentrations from blood samples taken from the tip of the tail were measured using a glucometer.

### 2.4. Intraperitoneal glucose tolerance test (IPGTT)

Glucose tolerance test is a widely used clinical test to diagnose glucose intolerance and T2DM (American Diabetes, 2007; Muniyappa et al., 2008). Food was removed a night before the test. The mice were injected with glucose (2 g/kg/ip, dissolved in saline). Blood glucose levels from blood samples taken from the tip of the tail were measured using a glucometer at 0, 30, 60, and 120 min after the bolus. The area under the concentration versus time curve (AUC glucose 0–120 min, mg/dl * minutes) was calculated.

### 2.5. Intraperitoneal insulin tolerance test (IPITT)

Mice were fasted for 4 h before the test. The mice were injected with insulin (0.75 U/kg/ip, dissolved in saline). Blood glucose levels from blood samples taken from the tip of the tail were measured using a glucometer at 0, 15, 30, 60, and 120 min after the bolus. The

**Table 1**
Diet composition.

| | Normal diet | High fat diet |
|---|---|---|
| Protein (kcal %) | 24.5 | 20 |
| Carbohydrate (kcal %) | 62.4 | 20 |
| Fat (kcal %) | 13.1 | 60 |

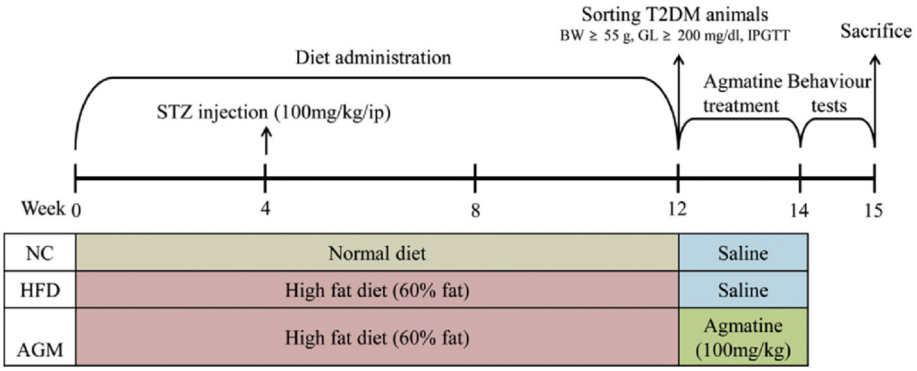


**Fig. 1. Timeline for the *in vivo* study**. Mice were randomly assigned into two groups and then fed either a normal diet (NC) or a high-fat diet (HFD) for 12 weeks. HFD-fed mice were injected once at week 4 with streptozotocin (STZ; 100 mg/kg/ip). Mice with a fasting serum glucose level >200 mg/dl, body weight >55 g, and impaired glucose tolerance were selected and then randomly divided into two groups: HFD mice treated with saline and HFD mice treated with agmatine (HFD + AGM; 100 mg/kg/ip) for 2 weeks. Behaviour tests were conducted prior to sacrifice.

area under the concentration versus time curve (AUC glucose 0–120 min, mg/dl * minutes) was calculated.

### 2.6. Behaviour tests

#### 2.6.1. Morris water maze (MWM)

The Morris water maze test was conducted for evaluating spatial learning and reference memory depending on hippocampus using a previously established protocol (Morris et al., 1982) with some modifications. Our test consisted of 4 days of training and a test session on day 6. Mice were transferred from their home cage to the behaviour room to adapt to the new environment for at least 30 min before each session. The apparatus consisted of a circular water pool (100 cm in diameter, 35 cm in height) that was filled with opaque water to a depth of 15.5 cm. A platform (5.5 cm in diameter, 14.5 cm in height) was placed at a fixed location. Four different figures were attached on the wall as visual cues. Each mouse received four trainings per day for 4 consecutive days. During each training session, the escape latency from the water to the platform was measured. All mice were allowed to find the platform for a maximum of 90 s. On day 5, a test session was conducted in which the mice were allowed to swim freely in the pool without the platform for 90 s. The time spent in the quadrant where the platform was previously located was measured.

#### 2.6.2. Nest building test

The nest building test was conducted after MWM for evaluating hippocampal function. The mice were moved into individual cages with a cotton pad (50 × 50 mm, 5 g). After 24 h, each nest was recorded and scored on a scale of 1–5 by five researchers according to the established criteria (Deacon, 2006). These criteria include scores for the shape of the nest and the amount of material used.

### 2.7. Tissue sample preparation

After the behaviour tests, the mice were transcardially perfused with saline and their brains were removed. Two hemispheres from each brain were randomly selected for either western blot or immunohistochemistry. Hemispheres for immunohistochemistry were incubated in 4% paraformaldehyde (PFA) for 24 h at 4 °C and then transferred to a 30% sucrose solution for 1 week. These hemispheres were embedded in medium (Tissue-Tek® O.C.T.™ Compound, Sakura Finetek USA, Inc., Torrance, CA, USA), cut into 20 μm slices on a cryostat, and stored at −20 °C until immunohistochemistry was performed. The hemispheres for western blot assay were placed in saline and carefully dissected. The hippocampus and cortex regions were immediately frozen in liquid nitrogen and stored until western blot assay.

### 2.8. Immunofluorescence

The sections were mounted on tissue slides and then permeabilized with 0.025% Triton X-100. The sections were blocked with 10% donkey serum at room temperature for 1 h. The sections were immunostained with primary antibodies against p-tau (Ser 202, Tyr 205, 1:200), Aβ (1:200), and *p*-GSK-3β (Ser9, 1:200) at 4 °C overnight. After the sections were washed with PBS (0.05% with Tween 20), FITC, or rhodamine-conjugated donkey anti-rabbit or anti-mouse antibody (1:200) was applied for 1 h at room temperature. The sections were mounted on tissue slides and then counter stained with DAPI. The tissues were visualized under a confocal microscope (Zeiss LSM 700, Carl Zeiss, Thornwood, NY, USA).

### 2.9. Western blot assay

The hippocampus and cortex were treated with lysis buffer containing inhibitor cocktails and isolated protein from the homogenizer (Dremel, Racine, WI, USA). The protein concentration was determined using the BCA method. A total of 50 μg of protein was separated on 6% or 10% SDS-PAGE gels and electrotransferred onto a PVDF membrane. After blocking the membrane with 5% bovine serum albumin, the membranes were reacted with primary antibodies that specifically detect IRS-1 (1:1000), p-IRS-1 (Tyr 632, 1:1000), Akt (1:1000), *p*-Akt (Ser473, 1:1000), *p*-GSK-3β (Ser9, 1:1000), GSK-3β (1:1000), p-tau (Ser 202, Tyr 205, 1:1000), Aβ (1:1000), TNF-α (1:1000), IL-1β (1:1000) and β-actin (1:2500) at 4 °C overnight. After washing with TBS (0.5% with Tween 20), the membranes were reacted with HRP-conjugated anti-mouse, anti-rabbit, or anti-goat IgG antibodies (1:3000) at room temperature for 1 h. After washing with TBS (0.5% with Tween 20), signals were observed using enhanced ECL reagents. The images were captured by the chemi-luminescent image analyzer (LAS 4000, Fujifilm, Tokyo, Japan).

### 2.10. Serum and tissue insulin ELISA assay

Serum insulin was measured with an insulin ELISA kit (ALPCO, Windham, NH, USA), and tissue insulin was measured with an insulin ELISA kit (Shibayagi, Gumma, Japan). We loaded 10 μL of each of the standard, control, and experimental samples into

appropriate wells. Then, we added 75 μL of enzyme conjugate (mouse monoclonal anti-insulin conjugated to biotin) into each well and incubated for 2 h at room temperature, shaking at 800 rpm on a microplate shaker. Microplates were washed six times with 350 μL of wash buffer. Then, we added 100 μL of substrate solution (tetramethylbenzidine) to each well and incubated the samples for 15 min at room temperature, shaking at 800 rpm on a microplate shaker. The enzymatic reaction was stopped by adding 100 μL of stop solution to each well, and absorbance was measured at 450 nm using a microplate reader.

### 2.11. Amyloid beta ELISA assay

Tissue amyloid beta was measured with an amyloid beta ELISA kit. Samples were prepared using 5 M guanidine HCl/50 mM Tris HCl solution with protease inhibitor cocktail containing AEBSF. Briefly, we loaded 100 μL of each of the standard, control, and experimental samples into appropriate wells and incubated the specimens for 2 h at room temperature. We then washed the microplate four times with 400 μL of wash buffer. Then, 100 μL of detection antibody was added into each well and incubated for 1 h at room temperature. The microplate was then washed four times with 400 μL of wash buffer. Then, we added 100 μL of HRP anti-rabbit antibody to each well and incubated the specimens for 30 min at room temperature. We then washed the microplate again four times with 400 μL of wash buffer. Then, we added 100 μL of stabilized chromogen to each well and incubated the specimens for 30 min at room temperature. The enzymatic reaction was stopped by adding 100 μL of stop solution to each well, and absorbance was determined at 450 nm using a microplate reader.

### 2.12. Serum analysis

Serum levels of total cholesterol and triglyceride were measured by chemistry analyzer, Fuji dri-chem 4000i (Fuji photo film, Tokyo, Japan) and Fuji dri-chem slides. Fuji dri-chem slide contains suitable enzymes for separating a factor that we wanted to measure from serum. 10 μL of sample was dropped onto each slide to induce enzymatic reaction, and then slides were read using Fuji dri-chem 4000i.

### 2.13. Statistical analysis

All experiments were repeated at least three times, and the data are expressed as the mean ± standard deviation (SD). Statistical analysis was performed by a one-way analysis of variance (ANOVA), followed by Tukey's post hoc analysis. Statistical significance was defined as $^{*}\ p \leq 0.05$ and $^{**}p \leq 0.01$ vs. NC.

## 3. Results

### 3.1. Agmatine treatment restores insulin sensitivity, reducing peripheral glucose intolerance, insulin intolerance, and serum triglyceride levels and increasing serum insulin levels in HFD-fed mice

To induce brain insulin resistance, 8-week-old ICR mice were fed a 60% high-fat diet for 12 weeks. As shown in Fig. 2, the high-fat diet induced significant weight gain (NC vs. HFD, average weight: week 0, 39.93 ± 0.86 mg vs. 40.68 ± 1.83 mg; week 12, 48.68 ± 4.22 mg vs. 66.69 ± 6.8 mg, Fig. 2A) and increased fasting serum glucose levels (NC: 155 ± 13.49 mg/dl vs. HFD: 522 ± 31.6 mg/dl at 14 weeks, Fig. 2B). Most importantly, glucose tolerance and insulin tolerance were significantly impaired in the HFD group, compared with the NC group (difference of 162 095 mg/dl*min in the AUC of the IPGTT between the HFD and NC mice, Fig. 2C and D; difference of 27 017.5 mg/dl*min in the AUC of the IPITT between the HFD and NC mice, Fig. 2E and F). One low-dose injection of STZ was used to mimic pancreas failure in the pathogenesis of T2DM; STZ evoked no significant damage to the pancreas (Supplementary Fig. 1). Despite normal pancreatic function, characteristics of T2DM and insulin resistance, including increases in body weight, fasting serum glucose level, glucose intolerance and insulin intolerance, were induced by 12 weeks of a high-fat diet.

After 2 weeks of agmatine treatment, glucose and insulin intolerance were significantly recovered ($p > 0.01$, HFD vs. HFD + AGM, Fig. 3F–I). While no significant difference in body weight or 4-hour fasting serum glucose levels were found (Fig. 3A and B), overnight fasting serum glucose levels were significantly lower (Fig. 3C).

Mouse serum insulin ELISA assay revealed that the high fat-diet increased serum insulin concentrations, compared with NC (Fig. 3D). Serum analysis showed that HFD mice had lower total cholesterol and higher triglyceride than NC, although agmatine treatment lowered triglyceride levels and increased total cholesterol level (Fig. 3E). Based on the results of IPGTT, IPITT, overnight fasting serum glucose level, insulin ELISA, and serum analysis, we can conclude that agmatine treatment restores insulin sensitivity in high-fat diet fed mice.

### 3.2. Agmatine treatment rescues reduced insulin signalling in the brain of HFD-fed mice

To evaluate the effect of agmatine on brain insulin resistance induced by the high-fat diet, the amount of insulin in the brain was measured by ELISA, and the expression levels of p-IRS-1 and *p*-Akt in both the cortex and the hippocampus were measured by western blot assay. As seen in Fig. 4, the amount of insulin and the protein expression levels of p-IRS-1 and *p*-Akt were significantly reduced in both the cortex and the hippocampus of the HFD mice (insulin, $p > 0.05$ vs. NC; p-IRS-1, $p > 0.05$ vs. NC; *p*-Akt, $p > 0.05$ vs. NC), compared with NC mice. However, HFD + AGM mice exhibited significantly higher levels of insulin, p-IRS-1, and *p*-Akt (insulin, $p > 0.05$ vs. HFD; p-IRS-1,$p > 0.05$ vs. HFD; *p*-Akt, $p > 0.05$ vs. HFD) in the cortex and the hippocampus of the mice. The amount of insulin and phosphorylated molecules in HFD + AGM mice was similar to those in NC mice in both the cortex (p-IRS-1, 93%, *p*-Akt, 166% as a percentage of NC) and the hippocampus (p-IRS-1, 94%; *p*-Akt, 127% as percentage of NC).

### 3.3. 3Agmatine treatment restores the phosphorylation of glycogen synthase kinase-3β in both the cortex and hippocampus of HFD-fed mice

Among the molecules downstream from insulin, glycogen synthase kinase-3β (GSK-3β) is well known to phosphorylate tau leading to production of neurofibrillary tangles and Alzheimer's disease. Normally, insulin downstream signals inhibit GSK-3β by phosphorylation at serine 9 so that GSK-3β cannot phosphorylate tau. Western blot assays and immunofluorescence were conducted to confirm the ability of agmatine to restore the phosphorylation of GSK-3β in mice with brain insulin resistance. As seen in Fig. 5A and B, the western blot assay revealed that the protein expression of *p*-GSK-3β was significantly decreased in both the cortex and the hippocampus in HFD mice, compared with NC mice ($p > 0.05$ vs. NC). However, the expression of *p*-GSK-3β was significantly higher in both the cortex and the hippocampus in HFD + AGM mice ($p > 0.05$ vs. HFD). The level of *p*-GSK-3β in HFD + AGM mice was similar to p- GSK-3β in NC mice in both the cortex (91% as a percentage of NC mice) and the hippocampus (95% as a percentage of

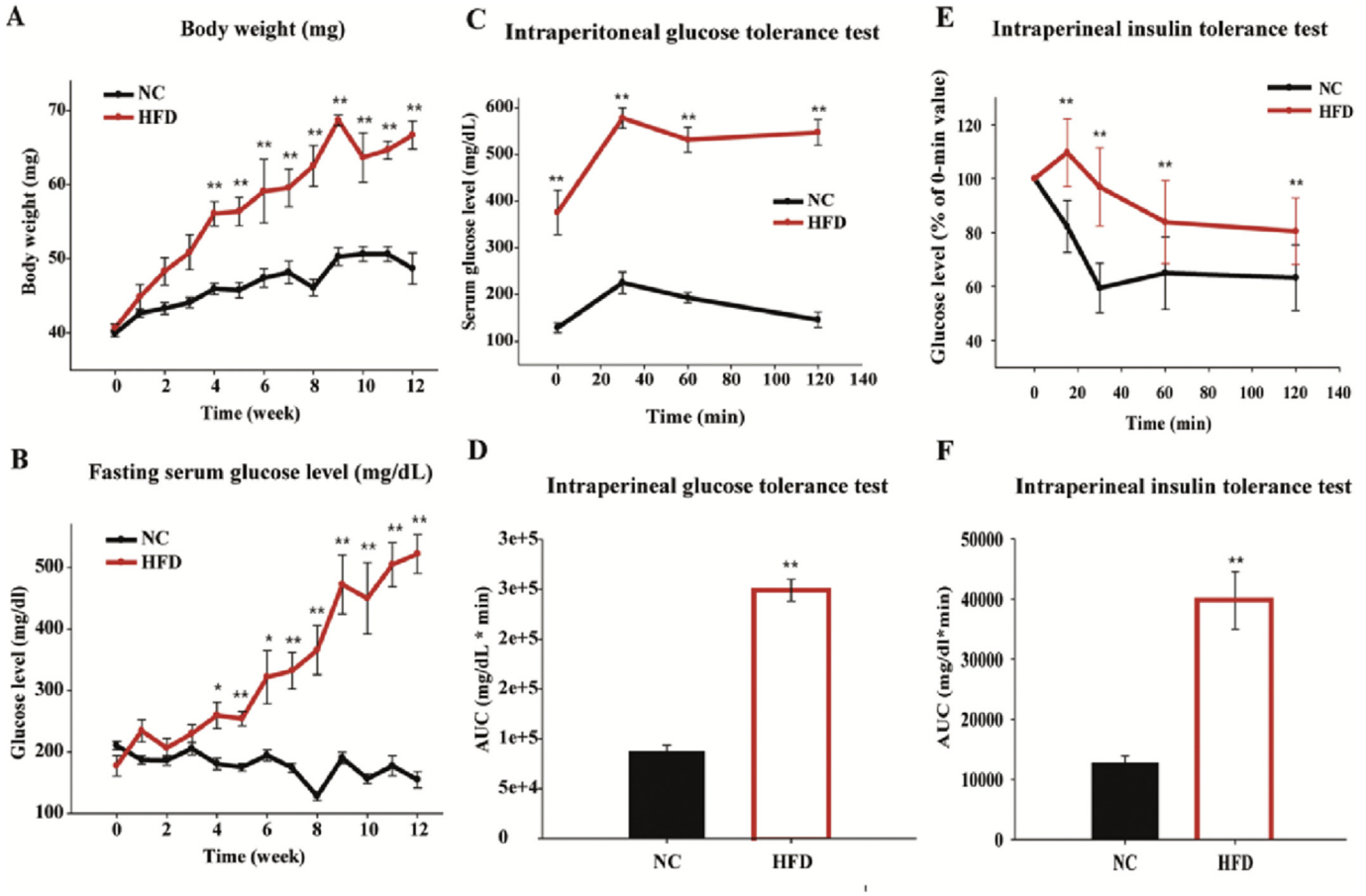


**Fig. 2. High-fat diet induces changes in weight, fasting serum glucose levels, glucose tolerance test, and insulin tolerance test**. (A) Changes in body weight in the high-fat diet (HFD) group and the normal diet (NC) group for 12 weeks. (B) Changes in fasting serum glucose level in the HFD and NC groups for 12 weeks. (C) Changes in glucose level during the intraperitoneal glucose tolerance test (IPGTT). (D) The area under the curve (AUC) of the glucose level during the IPGTT. (E) Changes in glucose level during the intraperitoneal insulin tolerance test (IPITT). (F) The area under the curve (AUC) of the glucose level during the IPITT.*$p < 0.05$, **$p < 0.01$.

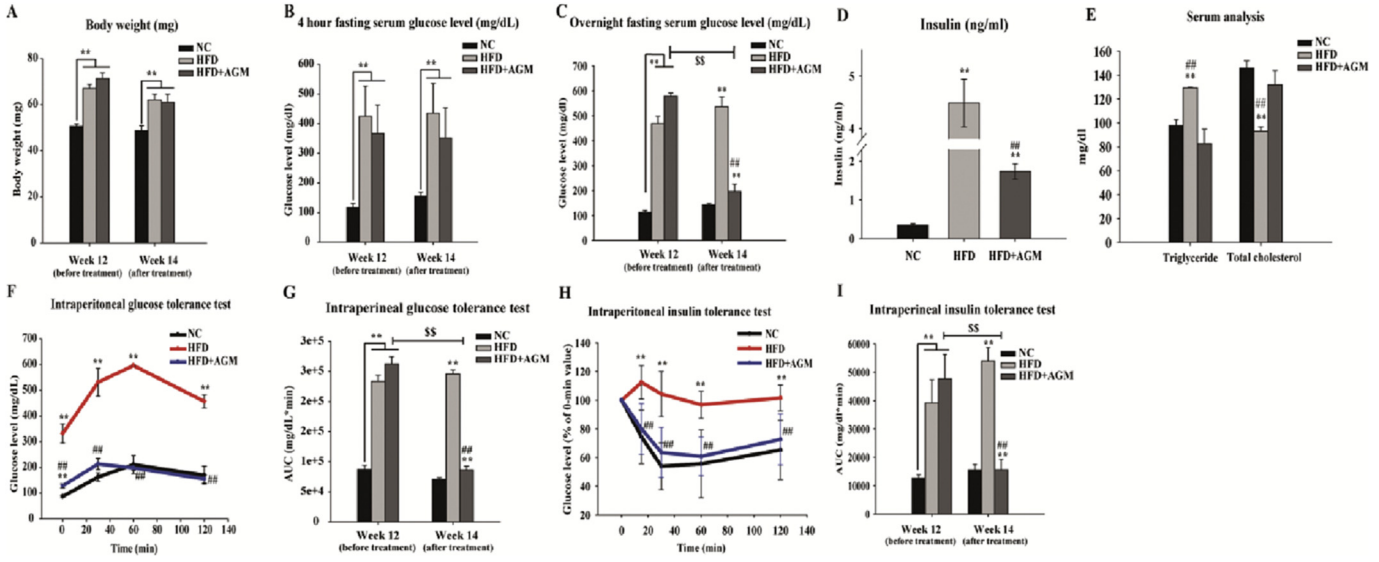


**Fig. 3. Agmatine treatment ameliorates glucose intolerance, insulin intolerance, overnight fasting serum glucose, insulin level, and triglyceride, but not body weight and 4-hours fasting serum glucose level, in high-fat diet-fed mice**. Comparison in the biochemical changes between week 12 (before agmatine treatment) and week 14 (after agmatine treatment). (A) Changes in body weight between week 12 and week 14. (B) Changes in 4-hour fasting serum glucose levels between week 12 and week 14. (C) Changes in overnight fasting serum glucose level between week 12 and week 14. (D) Amount of insulin at week 14 as measured by ELISA. (E) Serum analysis to measure triglyceride and total cholesterol levels at week 14. (F) Changes in glucose level during the intraperitoneal glucose tolerance test (IPGTT) at week 14. (G) Changes in the area under the curve (AUC) for glucose levels during the IPGTT between week 12 and week 14. (H) Changes in glucose level during the intraperitoneal insulin tolerance test (IPITT) at week 14. (I) Changes in the area under the curve (AUC) for glucose levels during the IPITT between week 12 and week 14. **$p < 0.01$ vs. NC, ##$p < 0.01$ vs. HFD + AGM, $$ $p < 0.01$ in HFD + AGM between 12 and 14 weeks.

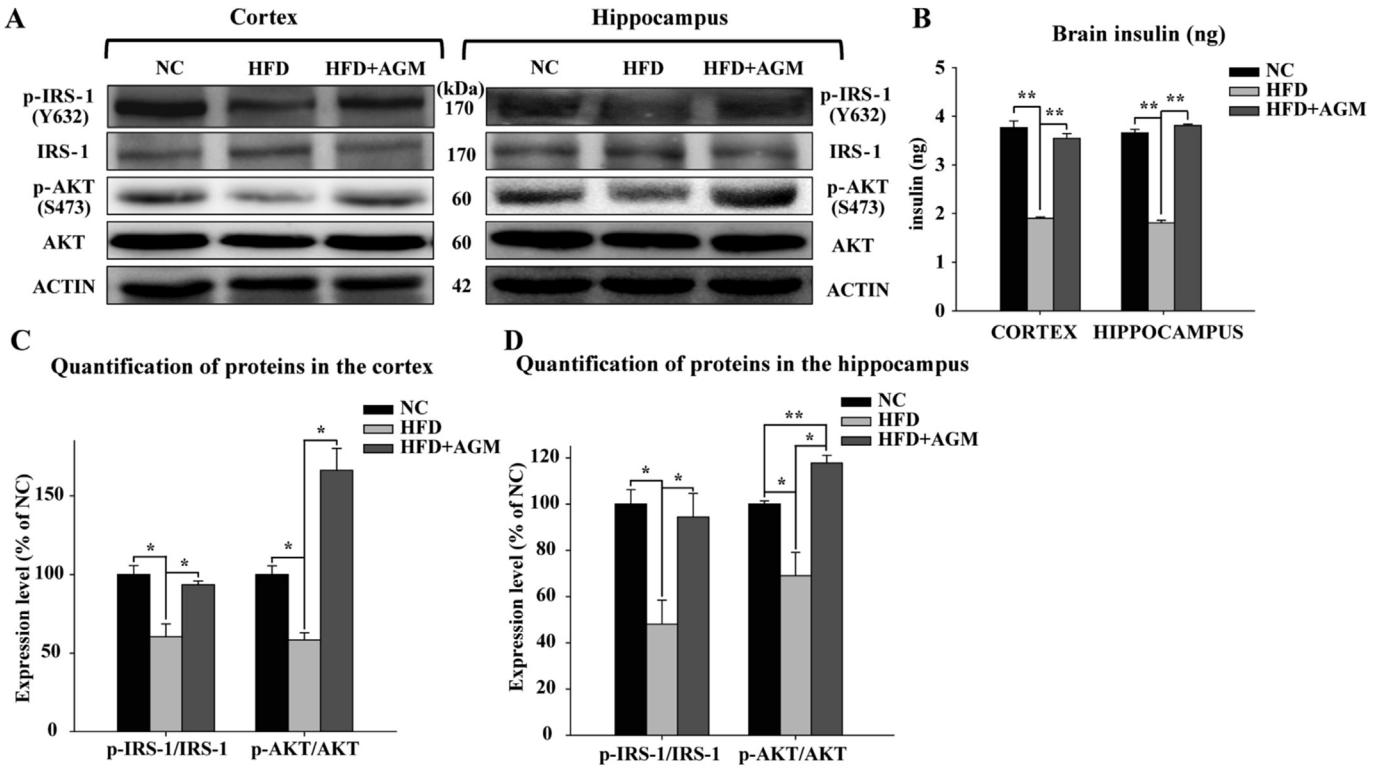


**Fig. 4. Agmatine increases the expression levels of insulin, p-IRS-1, and *p*-Akt in the cortex and the hippocampus of high-fat diet-fed mice**. (A) The effects of agmatine on the protein expression levels of p-IRS-1and *p*-Akt in the cortex and the hippocampus as measured by western blot assay. (B) The amount of insulin in the cortex and the hippocampus of the mice as measured by ELISA. (C) The quantification of p-IRS-1 and *p*-Akt in the cortex is expressed as a percentage of the levels observed in NC mice. (D) The quantification of p-IRS-1 and *p*-Akt in the hippocampus is expressed as a percentage of the levels observed in NC mice. $^{*}p < 0.05$, $^{**}p < 0.01$.

NC mice).

Immunofluorescence revealed that the expression of *p*-GSK-3β was significantly reduced in the cortex and the hippocampus of HFD mice, except in CA3 of the hippocampus (Fig. 5C–F) (frontal cortex, $p < 0.01$ vs. NC; lateral cortex, $p < 0.01$ vs. NC; DG, $p < 0.01$ vs. NC; CA1, $p < 0.01$ vs. NC; CA2, $p < 0.01$ vs. NC). However, repeated agmatine administration significantly restored the expression of *p*-GSK-3β in the cortex and the hippocampus (frontal cortex, $p < 0.01$ vs. HFD; lateral cortex, $p < 0.01$ vs. HFD; CA1, $p > 0.05$ vs. HFD; CA2, $p < 0.01$ vs. HFD; CA3, $p < 0.01$ vs. HFD), except in the dentate gyrus. These results are consistent with the western blot assay results (Fig. 5A and B).

### *3.4. Agmatine injection attenuates the phosphorylation of tau in both the cortex and hippocampus of high-fat diet-fed mice*

Western blot assay and immunohistochemistry were conducted to examine whether the ability of agmatine to increase the phosphorylation of GSK-3β leads to a reduction of phosphorylated tau in diabetic mice with brain insulin resistance. The western blot assay revealed that the expression of p-tau was increased in HFD mice, compared with NC mice, in both the cortex and the hippocampus (cortex, $p < 0.01$ vs. NC; hippocampus, $p < 0.01$ vs. NC). However, the expression of p-tau was significantly reduced in HFD + AGM mice, compared with HFD mice, in both the cortex and the hippocampus (cortex, $p < 0.01$ vs. HFD; hippocampus, $p < 0.01$ vs. HFD) (Fig. 6A and B).

Immunofluorescence revealed that the number of positive p-tau spots was significantly increased in HFD mice, compared with NC mice (frontal cortex, $p < 0.01$ vs. NC; lateral cortex, $p < 0.05$ vs. NC). Repeated treatment with agmatine significantly lowered the expression of p-tau in the cortex (frontal cortex, $p < 0.01$ vs. HFD; lateral cortex, $p < 0.05$ vs. HFD) (Fig. 6C and D). Similarly, the number of positive spots of p-tau were significantly higher in the DG and CA3 regions of the hippocampus in HFD mice, compared with NC mice (DG, $p < 0.01$ vs. NC; CA3, $p<0.01$ vs. NC) (Fig. 6D, F). However, the repeated agmatine administration significantly lowered the expression of p-tau in the hippocampus (DG, $p < 0.01$ vs. HFD; CA1, $p < 0.05$ vs. HFD; CA2, $p < 0.01$ vs. HFD; CA3, $p < 0.01$ vs. HFD) (Fig. 6E and F).

### *3.5. Agmatine treatment reduces the accumulation of amyloid beta in both the cortex and the hippocampus of high-fat diet-fed mice*

Western blot assay, immunohistochemistry, and tissue ELISA were conducted to investigate whether the agmatine-mediated activation of blunted insulin signals in the brain reduces the accumulation of Aβ. As shown in Fig. 7A B, G, the western blot assay and tissue ELISA revealed that the amount of Aβ was increased in HFD mice, compared with NC mice (hippocampus, $p < 0.01$ vs. NC; cortex, $p < 0.01$ vs. NC). However, the expression of Aβ was significantly decreased in HFD + AGM mice, compared with HFD mice (hippocampus, $p < 0.01$ vs. HFD; cortex, $p < 0.01$ vs. HFD). All species of amyloid beta protein bands are presented in Supplementary Fig. 2.

Immunofluorescence revealed that the expression of Aβ was significantly higher in HFD mice, compared with NC mice (frontal cortex, $p < 0.01$ vs. NC; lateral cortex, $p < 0.05$ vs. NC). Repeated treatment with agmatine significantly lowered the expression of Aβ in the cortex (frontal cortex, $p < 0.01$ vs. HFD; lateral cortex, $p < 0.05$ vs. HFD) (Fig. 6C and D). The number of positive spots of Aβ were significantly increased in the hippocampus of HFD mice, except in

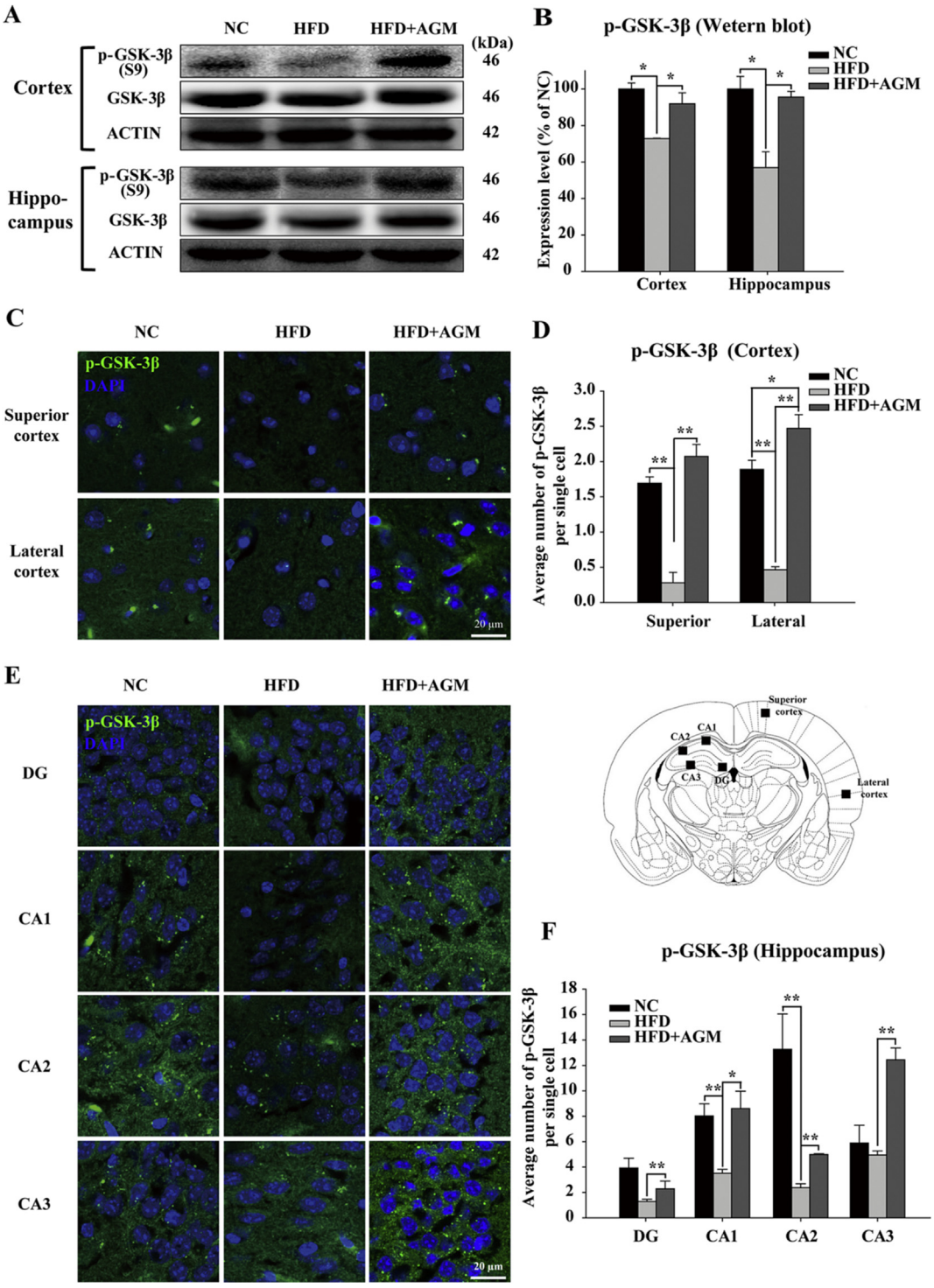


**Fig. 5. Agmatine increases the phosphorylation of GSK-3β in the cortex and the hippocampus of high-fat diet-fed mice**. (A) The effect of agmatine on the protein expression of *p*-GSK-3β in the cortex and the hippocampus as measured by western blot assay. (B) The quantification of *p*-GSK-3β in the cortex and the hippocampus is expressed as a percentage of the level observed in NC mice. (C) Fluorescence images of *p*-GSK-3β in the cortex. (D) The average number of positive spots of *p*-GSK-3β per single cell of the cortex is expressed. (E) Fluorescence images of *p*-GSK-3β in the hippocampus. (F) The average number of positive spots of *p*-GSK-3β per single cell of the hippocampus is expressed. $^{*}p < 0.05$, $^{**}p < 0.01$. The scale bars represent 20 μm. DG: dentate gyrus; CA1: CornuAmmonis 1; CA2: CornuAmmonis 2; CA3: CornuAmmonis 3.

the DG (CA1, $p < 0.01$ vs. NC; CA2, $p < 0.01$ vs. NC; CA3, $p < 0.01$ vs. NC). Repeated agmatine administration significantly lowered the expression of Aβ in the hippocampus, except in the DG (CA1, $p < 0.01$ vs. HFD; CA2, $p < 0.01$ vs. HFD; CA3, $p < 0.01$ vs. HFD) (Fig. 6E and F).

### *3.6. Agmatine administration improves learning and memory function in high-fat diet-fed mice*

Behaviour tests were conducted to determine whether the reduction in the expression levels of Aβ and p-tau by agmatine

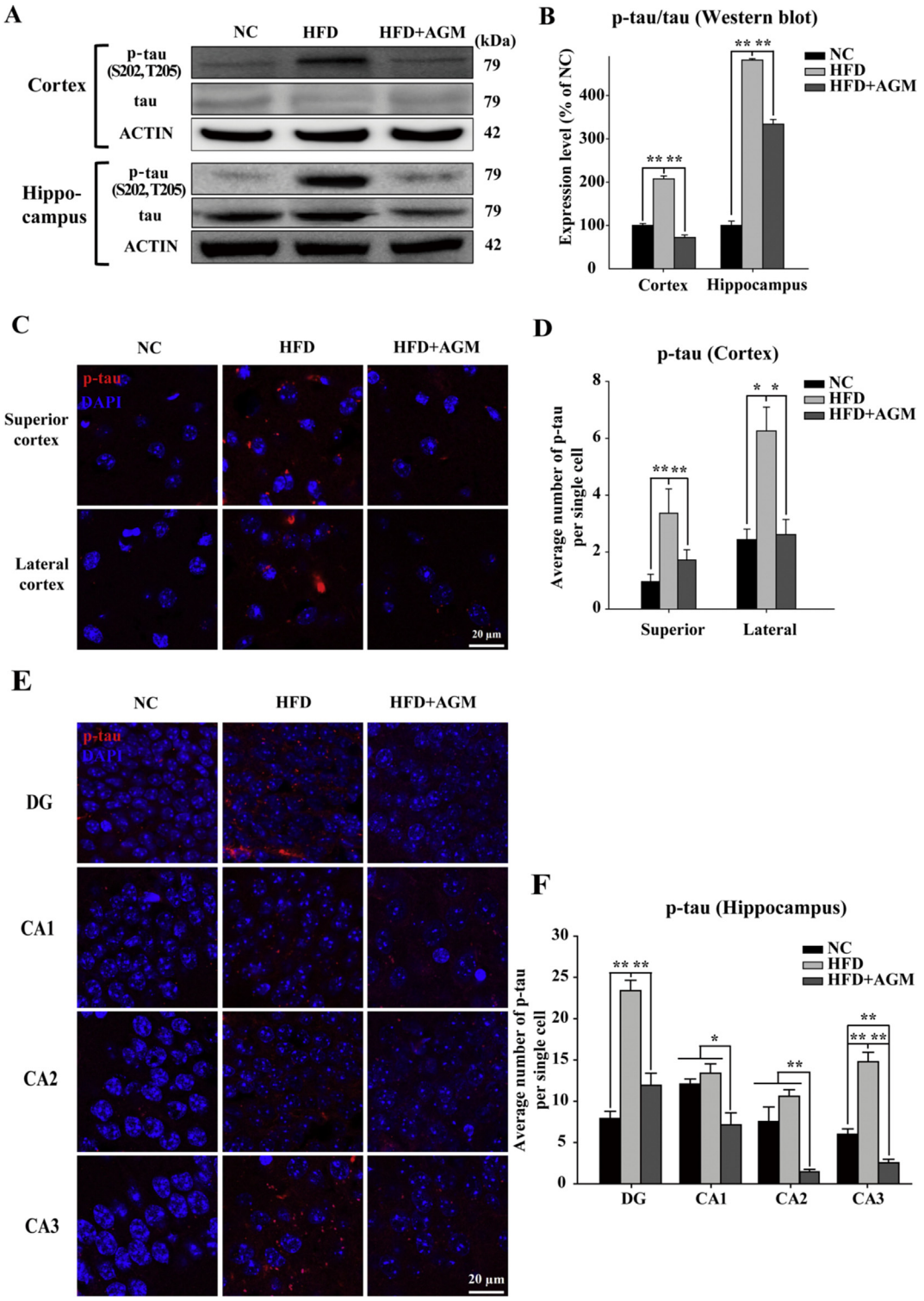


**Fig. 6. Agmatine reduces the accumulation of p-tau in the cortex and the hippocampus of high-fat diet-fed mice**. (A) The effect of agmatine on the protein expression of p-tau in the cortex and the hippocampus as measured by western blot assay. (B) The quantification of the amount of p-tau from the cortex and the hippocampus is expressed as a percentage of the level observed in NC mice. (C) Immunofluorescence images of p-tau in the cortex. (D) The average number of positive spots of p-tau per single cell in the cortex is expressed. (E) Immunofluorescence images of p-tau in the hippocampus. DG; dentate gyrus, CA1; CornuAmmonis 1, CA2; CornuAmmonis 2, CA3; CornuAmmonis 3. (F) The average number of positive spots of p-tau per single cell in the hippocampus is expressed. $^{*}p < 0.05$, $^{**}p < 0.01$. The scale bars represent 20 μm.

leads to an improvement in learning and memory function. Morris water maze test is conducted to evaluate spatial learning and preference memory depending on hippocampus. In addition, MWM has been shown that there is involvement of the entorhinal and perihinal cortices, as well as involvement of the prefrontal cortex, the cingulated cortex, the neostriatum, and perhaps even the cerebellum in a more limited way. In the MWM, a significant increase in escape latency on the last day of training was observed

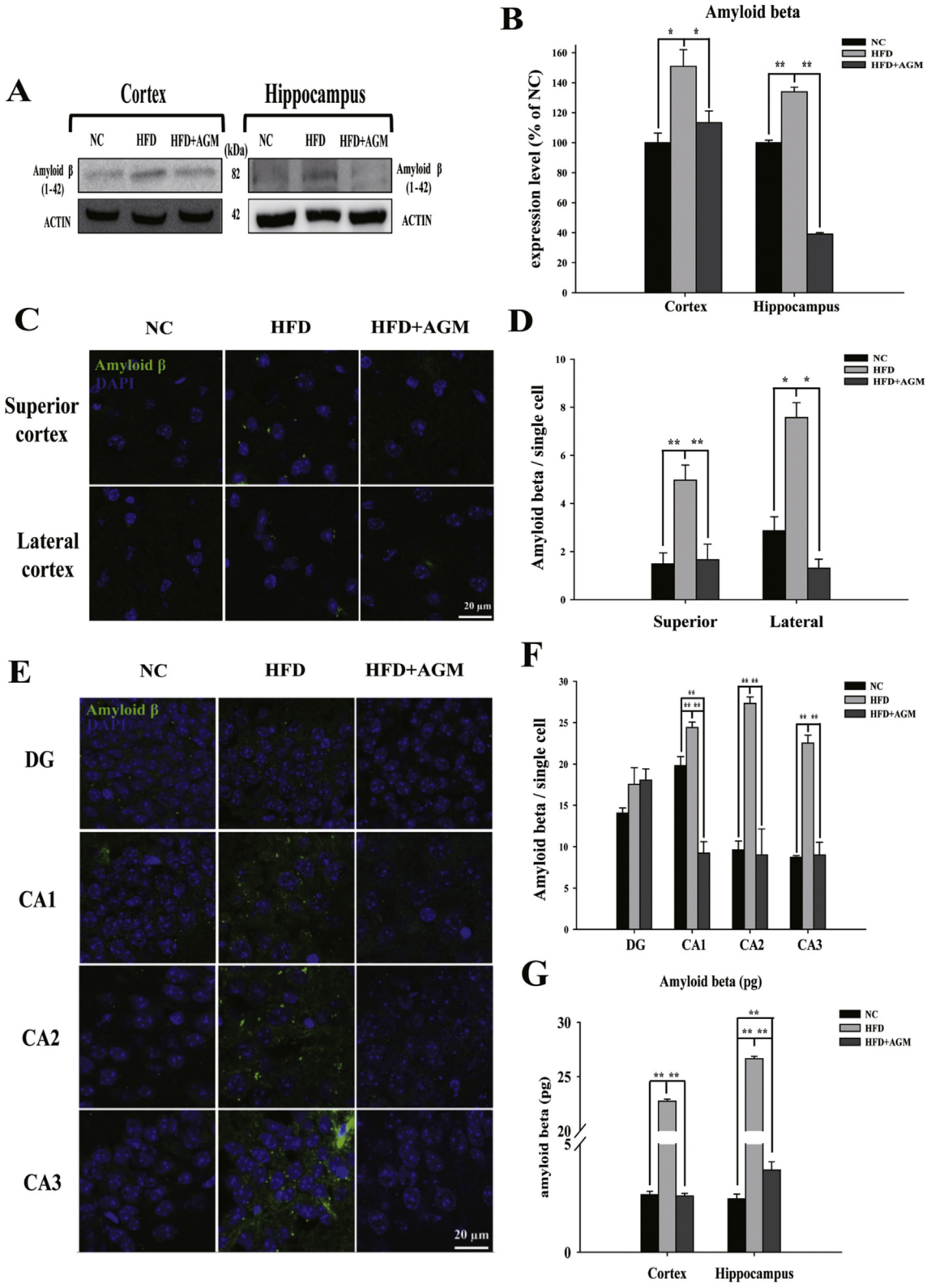


**Fig. 7. Agmatine reduces the accumulation of amyloid beta in the cortex and the hippocampus of high-fat diet-fed mice**. (A) The effect of agmatine on Aβ expression in the cortex and hippocampus as measured by western blot assay. (B) The quantification of Aβ from the cortex and the hippocampus is expressed as a percentage of the level observed in NC mice. (C) Immunofluorescence images of Aβ in the cortex. (D) The average number of positive spots of Aβ per single cell in the cortex is expressed. (E) Immunofluorescence images of Aβ in the hippocampus. (F) The average number of positive spots of Aβ per single cell in the hippocampus is expressed. (G) The amount of amyloid beta in the cortex and the hippocampus as measured by ELISA. $^{*}p < 0.05$, $^{**}p < 0.01$. The scale bars represent 20 μm. DG: dentate gyrus; CA1: CornuAmmonis 1; CA2: CornuAmmonis 2; CA3: CornuAmmonis 3.

in HFD mice, compared with NC mice ($p < 0.05$ vs. NC) (Fig. 8A). HFD mice spent significantly less time in the quadrant where the platform was located during the test, compared with NC mice ($p < 0.01$ vs. NC) (Fig. 8B). However, the amount of time spent in the platform quadrant was significantly longer in HFD + AGM mice, compared with HFD mice ($p < 0.01$ vs. HFD) (Fig. 8B).

Nest building test is conducted to evaluate hippocampal function, as some publications report that lesions of the medial preoptic area, septum, or hippocampus impair nesting behaviour. HFD mice received lower scores on the nest building test, compared with NC mice ($p < 0.01$ vs. NC). However, HFD + AGM mice received significantly higher scores than HFD mice ($p < 0.01$ vs. HFD) (Fig. 8C).

Collectively, agmatine improved hippocampal functions, such as learning and memory, induced by high-fat diet through the activation of insulin signalling in type 2 diabetic mice with AD-like alterations characterized by brain insulin resistance (Fig. 9).

## 4. Discussion

In the present study, we demonstrated the effect of agmatine on AD-like alterations in patients with T2DM characterized by brain insulin resistance. Agmatine administration improved insulin actions and rescued the reduced expressions of p-IRS-1, *p*-Akt, and *p*-GSK-3β in the brain of high-fat diet-fed mice. Agmatine treatment reduced the amounts of Aβ and p-tau accumulation in the brain, and improved impairments in learning and memory functions in high-fat diet-fed mice.

There are two types of therapeutics of determine, insulin sensitizers and drugs effective for insulin production. The latter ones increase amounts of insulin, although agmatine did not increase serum insulin levels (Fig. 3D). Insulin sensitizer is effective for regulating pre-prandial serum glucose levels, not post-prandial serum glucose levels, and agmatine showed coherent action as shown in Fig. 3B and C. The reductions of serum insulin level, decreases in overnight fasting serum glucose level, and improvement

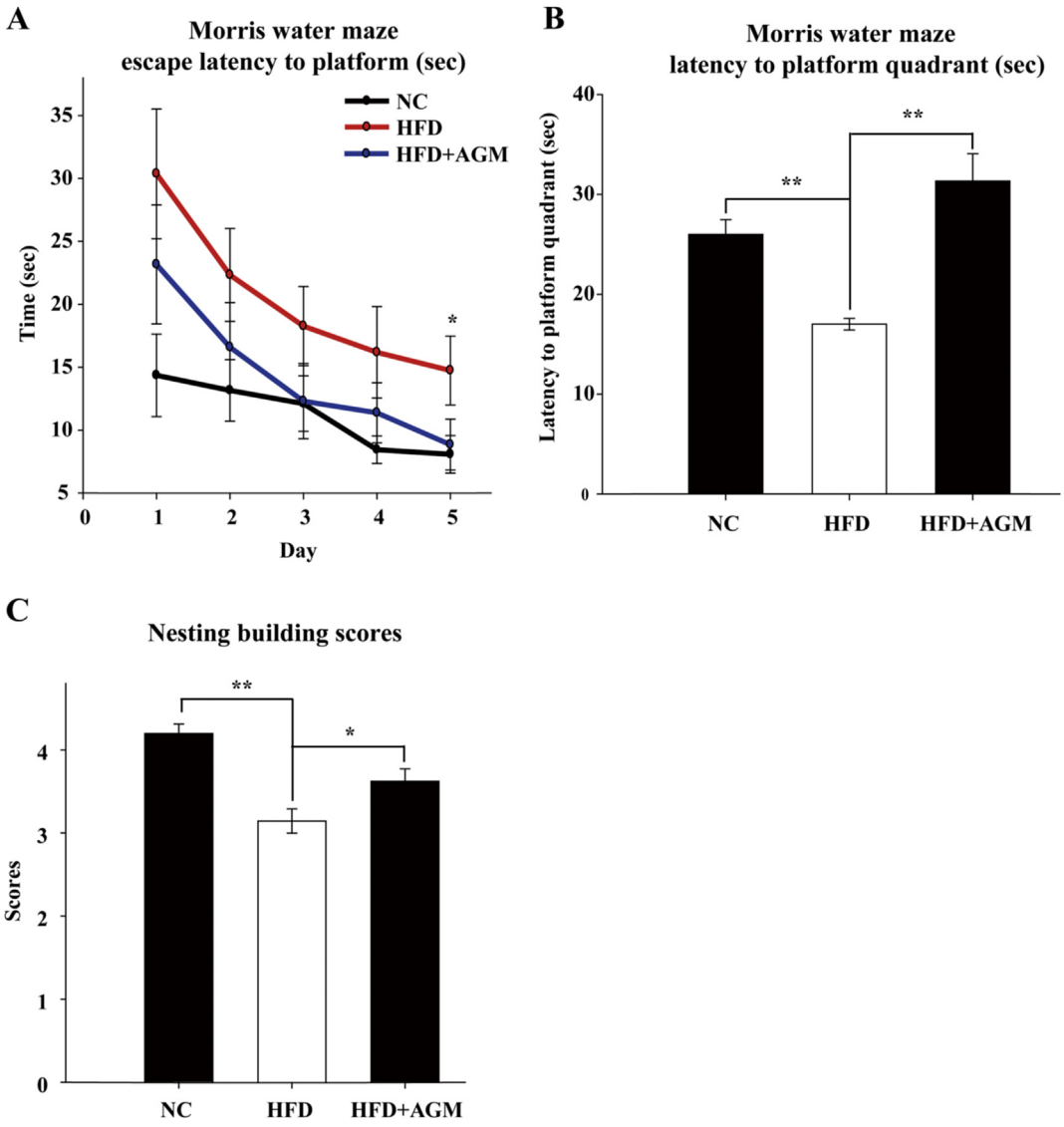


**Fig. 8. Agmatine improves learning, memory, and nesting function in high-fat diet fed mice**. (A) The mean escape latency over 5 days of training on the Morris water maze (MWM). *$p < 0.05$ vs. NC. (B) The mean time spent in the quadrant where the platform was located during the test session. (C) Nest building scores were based on the amount of material used and the shape of the nest. *$p < 0.05$, **$p < 0.01$.

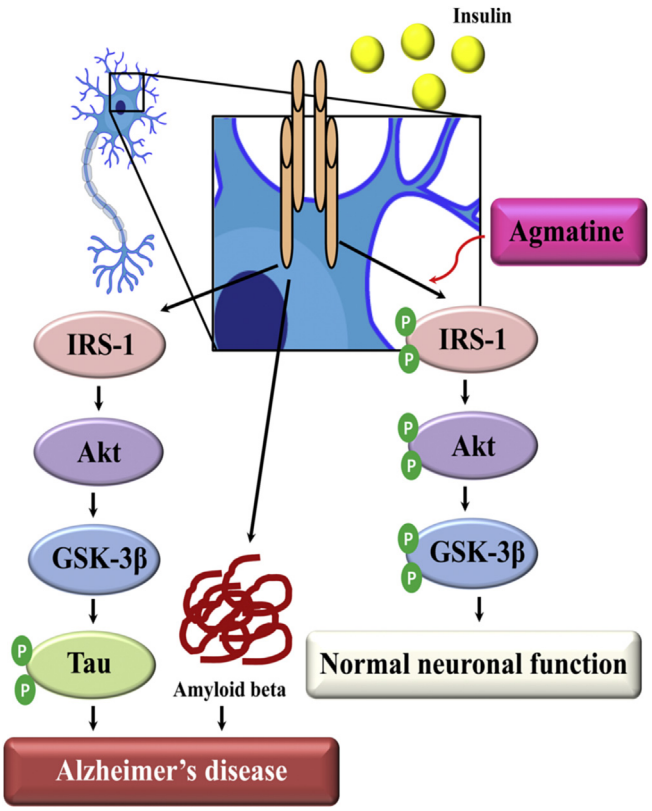


**Fig. 9. The effect of agmatine on brain insulin resistance**. Type 2 diabetes induces Alzheimer's disease-like alterations through blunted insulin signalling in the brain as it leads to the accumulation of Aβ, the phosphorylation of tau, and cognitive decline. However, agmatine activates the insulin signals in the diabetic mice with AD-like alterations characterized by brain insulin resistance to restore normal brain function. Agmatine reverses the Alzheimer's disease-like alterations induced by type 2 diabetes.

of insulin tolerance and glucose tolerance in the agmatine treated group indicated that agmatine improves insulin sensitivity. According to some research, agmatine improves insulin sensitivity by activation of I2-imidazolin receptors in adrenal gland in diabetic animal models (Chang et al., 2010; Hwang et al., 2005; Ko et al., 2008; Su et al., 2009). Accordingly, we suggest that agmatine exerts anti-diabetic effects by improving insulin sensitivity. In addition that, high-fat diet lowered total cholesterol while triglyceride level was increased by high-fat diet (Fig. 3E), suggesting triglyceride takes up most cholesterol in HFD mice. However, agmatine treated mice showed high level of total cholesterol and low level of triglyceride, meaning most of cholesterol could be LDL, not triglyceride. According to a paper, which has similar experimental design with ours, 12 weeks of 60% high-fat diet caused increase in triglyceride and LDL but decrease in HDL (Sharawy et al., 2016). However, 3 weeks of agmatine treatment reduced triglyceride and LDL. In addition to total cholesterol and triglyceride measurement, we could say animals used in present study would show similar changes in LDL and HDL with that reference paper.

Brain insulin resistance was induced by 12 weeks of a high-fat diet, and was characterized by blunted insulin signal transductions as observed in the expression levels of p-IRS-1, *p*-Akt, and *p*-GSK-3β (Figs. 4 and 5) and decreased insulin levels (Fig. 4B). Brain insulin resistance leads to both Aβ plaque formation and tau hyperphosphorylation (Kim and Feldman, 2012). Insulin inhibits the accumulation of Aβ via the stimulation of Aβ extracellular secretion (de la Monte, 2012; Gasparini et al., 2001; Watson et al., 2003). Insulin resistance induces oxidative stress and neuroinflammation, which promotes Aβ accumulation and toxicity (Pratico et al., 2001). Although GSK-3β phosphorylates tau, the phosphorylation of GSK-3β at serine 9 by insulin inhibits its action on tau. Therefore, a reduced insulin signal increases GSK-3β activity, leading to tau phosphorylation (Balaraman et al., 2006; Clodfelder-Miller et al., 2005; Takashima, 2006). In our study, the expression levels of Aβ and p-tau were increased, and neuroinflammation developed in the brain of mice in the high-fat diet group (Figs. 6 and 7, Supplementary Fig. 3), which is consistent with previous findings.

According to prior reports, T2DM affects cognitive processes, such as memory and executive function (Sims-Robinson et al., 2010). The hippocampus, which has the highest concentration of insulin receptors in the brain (Freude et al., 2009; Gammeltoft et al., 1985), is vulnerable to insulin resistance. A high-fat diet increases hippocampal oxidative stress, which reduces NF-E2-related factor 2 (Nrf2) signalling (Morrison et al., 2010), causes mitochondrial homeostasis deficiency (Petrov et al., 2015), and impairs hippocampus-dependent memory function (McNeilly et al., 2011). The MWM test is used to evaluate spatial memory depends primarily on the hippocampus. In our study, high-fat diet-fed mice displayed spatial memory impairment (Fig. 8 A,B), which is consistent with previous findings.

The deterioration of activities of daily living is an early sign of AD (Filali et al., 2012; Wesson and Wilson, 2011). In mice, injuries to the cortex and hippocampus can affect nesting behaviour (Deacon et al., 2002, 2003). Nest building ability is negatively correlated with Aβ accumulation in the brain (Wesson and Wilson, 2011). In our study, nest building function was impaired in HFD mice (Fig. 9C), which suggests that brain insulin resistance induced impairment of brain function.

The expression levels of p-IRS-1, *p*-Akt, and *p*-GSK-3β were increased in the brain of the HFD-AGM mice up to similar levels as those observed in NC mice. These results indicate that the insulin signals were being transmitted and phosphorylating IRS-1, Akt, and GSK-3β in the brain of the type 2 diabetic mice with AD-like alterations characterized by brain insulin resistance. Following the activation of the blunted insulin signals in the brain, treatment with agmatine significantly reduced Aβ and p-tau and improved memory function, which indicates that agmatine treatment reversed the AD-like alterations in high-fat diet-fed mice.

The increased expression of p-IRS-1 in the brain by agmatine treatment is a novel finding of this study. It has been reported that agmatine prevents memory deficits via the activation of ERK, Akt, and GSK-3β (Moosavi et al., 2012, 2014). Our result adds to this previous work by showing that agmatine activates not only Akt and GSK-3β but also their upstream signal regulator IRS-1.

Among the molecules activated by insulin receptor kinase, members of the IRS family recruit downstream signalling molecules, including phosphatidylinositol 3-dinase (PI3K) (Saltiel and Kahn, 2001). The phosphorylation of the tyrosine residues of IRS-1 promotes the metabolic functions of insulin, whereas the dephosphorylation of tyrosine and the phosphorylation of the serine/threonine residues dissociate IRS-1 from the insulin receptor and reduce insulin signalling (Kapogiannis et al., 2015). Many inducers of insulin resistance activate IRS serine kinases. Among these inducers, there are two kinds of serine kinases. One type of serine kinase is related to insulin signalling and includes kinases, such as the mammalian target of rapamycin (mTOR)/S6K1 and mitogen-activated protein kinase (MAPK). The other type of serine kinase is activated along unrelated pathways, and includes kinases, such as GSK-3β and c-Jun NH2-terminal kinase (JNK) (Ozcan et al., 2004). Physical exercise or pharmacological chemicals, such as thiazolidinedione (TZD) and metformin, improve insulin action via the inhibition of iNOS and mTOR/S6K1 signalling (Marette, 2008;

Pilon et al., 2004). Agmatine reduces the phosphorylation of JNK (Hong et al., 2007; Kim et al., 2015) and iNOS (Mun et al., 2010; Wang et al., 2010) under severe conditions, such as hypoxia, stroke, and traumatic injury. Therefore, agmatine might reduce the phosphorylation of iNOS and JNK in the brain of the T2DM mice with AD-like alterations characterized by brain insulin resistance to activate IRS-1.

The rescue of the blunted insulin signal in the hippocampus and the cortex by agmatine revived hippocampus-dependent memory function and cortex- and hippocampus-dependent nest building ability. HFD + AGM mice performed better on the MWM test than NC mice. Another reason why agmatine improves hippocampus-dependent spatial learning is that agmatine could be able to function as a neurotransmitter. The amount of agmatine is reduced in the superior frontal gyrus, cerebellum, and hippocampus of AD patients and AD rats (Liu et al., 2008a, 2014). Spatial learning enhances agmatine level in the hippocampus and the cortex (Leitch et al., 2011; Liu et al., 2008b). It is, therefore, possible that agmatine functioned as a neurotransmitter in this study to improve learning and memory function in the hippocampus.

Further studies are needed to confirm the direct relationship between brain insulin resistance and agmatine. Since agmatine was injected intraperitoneally, it is unclear whether AD-like alterations were rescued by agmatine directly or by recovering T2DM. An agmatine treatment in neuronal insulin resistance *in vitro* model could be helpful for clarifying the direct functions of agmatine on brain insulin resistance.

In conclusion, this study suggests that agmatine has the potential to rescue AD-like alterations in T2DM mice characterized by brain insulin resistance via the regulation of IRS-1, Akt, and GSK-3β. Agmatine attenuates AD-like alterations caused by brain insulin resistance by reducing Aβ and p-tau, and improves impaired hippocampal functions, such as learning and memory, via the activation of blunted insulin signal transduction in the brain (Fig. 9).

## Acknowledgement

This study was supported by a grant from the Korean Health Technology R&D Project (HI14C2173), Ministry of Health and Welfare, Republic of Korea.

## Appendix A. Supplementary data

Supplementary data related to this article can be found at http://dx.doi.org/10.1016/j.neuropharm.2016.10.029.

## References

Ahn, S.S., Kim, S.H., Lee, J.E., Ahn, K.J., Kim, D.J., Choi, H.S., Kim, J., Shin, N.Y., Lee, S.K., 2014. Effects of agmatine on blood-brain barrier stabilization assessed by permeability MRI in a rat model of transient cerebral ischemia. AJNR Am. J. Neuroradiol. 36 (2), 283–288.
American Diabetes, A., 2007. Diagnosis and classification of diabetes mellitus. Diabetes Care 30 (Suppl. 1), S42–S47.
Arnold, S.E., Lucki, I., Brookshire, B.R., Carlson, G.C., Browne, C.A., Kazi, H., Bang, S., Choi, B.R., Chen, Y., McMullen, M.F., Kim, S.F., 2014. High fat diet produces brain insulin resistance, synaptodendritic abnormalities and altered behavior in mice. Neurobiol. Dis. 67, 79–87.
Arteni, N.S., Lavinsky, D., Rodrigues, A.L., Frison, V.B., Netto, C.A., 2002. Agmatine facilitates memory of an inhibitory avoidance task in adult rats. Neurobiol. Learn Mem. 78, 465–469.
Balaraman, Y., Limaye, A.R., Levey, A.I., Srinivasan, S., 2006. Glycogen synthase kinase 3beta and Alzheimer's disease: pathophysiological and therapeutic significance. Cell Mol. Life Sci. 63, 1226–1235.
Belfiore, A., Frasca, F., Pandini, G., Sciacca, L., Vigneri, R., 2009. Insulin receptor isoforms and insulin receptor/insulin-like growth factor receptor hybrids in physiology and disease. Endocr. Rev. 30, 586–623.
Bhutada, P., Mundhada, Y., Humane, V., Rahigude, A., Deshmukh, P., Latad, S., Jain, K., 2012. Agmatine, an endogenous ligand of imidazoline receptor protects against memory impairment and biochemical alterations in streptozotocin-induced diabetic rats. Prog. Neuropsychopharmacol. Biol. Psychiatry 37, 96–105.
Byrne, F.M., Cheetham, S., Vickers, S., Chapman, V., 2015. Characterisation of pain responses in the high fat diet/streptozotocin model of diabetes and the analgesic effects of antidiabetic treatments. J. Diabetes Res. 2015, 752481.
Chang, C.H., Wu, H.T., Cheng, K.C., Lin, H.J., Cheng, J.T., 2010. Increase of beta-endorphin secretion by agmatine is induced by activation of imidazoline I(2A) receptors in adrenal gland of rats. Neurosci. Lett. 468, 297–299.
Clodfelder-Miller, B., De Sarno, P., Zmijewska, A.A., Song, L., Jope, R.S., 2005. Physiological and pathological changes in glucose regulate brain Akt and glycogen synthase kinase-3. J. Biol. Chem. 280, 39723–39731.
Craft, S., Watson, G.S., 2004. Insulin and neurodegenerative disease: shared and specific mechanisms. Lancet Neurol. 3, 169–178.
Cui, H., Lee, J.H., Kim, J.Y., Koo, B.N., Lee, J.E., 2012. The neuroprotective effect of agmatine after focal cerebral ischemia in diabetic rats. J. Neurosurg. Anesthesiol. 24, 39–50.
de la Monte, S.M., 2012. Brain insulin resistance and deficiency as therapeutic targets in Alzheimer's disease. Curr. Alzheimer Res. 9, 35–66.
Deacon, R.M., 2006. Assessing nest building in mice. Nat. Protoc. 1, 1117–1119.
Deacon, R.M., Croucher, A., Rawlins, J.N., 2002. Hippocampal cytotoxic lesion effects on species-typical behaviours in mice. Behav. Brain Res. 132, 203–213.
Deacon, R.M., Penny, C., Rawlins, J.N., 2003. Effects of medial prefrontal cortex cytotoxic lesions in mice. Behav. Brain Res. 139, 139–155.
Edwards, L.M., Murray, A.J., Holloway, C.J., Carter, E.E., Kemp, G.J., Codreanu, I., Brooker, H., Tyler, D.J., Robbins, P.A., Clarke, K., 2011. Short-term consumption of a high-fat diet impairs whole-body efficiency and cognitive function in sedentary men. FASEB J. 25, 1088–1096.
Filali, M., Lalonde, R., Theriault, P., Julien, C., Calon, F., Planel, E., 2012. Cognitive and non-cognitive behaviors in the triple transgenic mouse model of Alzheimer's disease expressing mutated APP, PS1, and Mapt (3xTg-AD). Behav. Brain Res. 234, 334–342.
Freude, S., Schilbach, K., Schubert, M., 2009. The role of IGF-1 receptor and insulin receptor signaling for the pathogenesis of Alzheimer's disease: from model organisms to human disease. Curr. Alzheimer Res. 6, 213–223.
Gammeltoft, S., Fehlmann, M., Van Obberghen, E., 1985. Insulin receptors in the mammalian central nervous system: binding characteristics and subunit structure. Biochimie 67, 1147–1153.
Gasparini, L., Gouras, G.K., Wang, R., Gross, R.S., Beal, M.F., Greengard, P., Xu, H., 2001. Stimulation of beta-amyloid precursor protein trafficking by insulin reduces intraneuronal beta-amyloid and requires mitogen-activated protein kinase signaling. J. Neurosci. 21, 2561–2570.
Gupta, A., Bisht, B., Dey, C.S., 2011. Peripheral insulin-sensitizer drug metformin ameliorates neuronal insulin resistance and Alzheimer's-like changes. Neuropharmacology 60, 910–920.
Haan, M.N., 2006. Therapy Insight: type 2 diabetes mellitus and the risk of late-onset Alzheimer's disease. Nat. Clin. Pract. Neurol. 2, 159–166.
Hong, S., Lee, J.E., Kim, C.Y., Seong, G.J., 2007. Agmatine protects retinal ganglion cells from hypoxia-induced apoptosis in transformed rat retinal ganglion cell line. BMC Neurosci. 8, 81.
Hwang, S.L., Liu, I.M., Tzeng, T.F., Cheng, J.T., 2005. Activation of imidazoline receptors in adrenal gland to lower plasma glucose in streptozotocin-induced diabetic rats. Diabetologia 48, 767–775.
Jayaraman, A., Pike, C.J., 2014. Alzheimer's disease and type 2 diabetes: multiple mechanisms contribute to interactions. Curr. Diab Rep. 14, 476.
Jiang, L.Y., Tang, S.S., Wang, X.Y., Liu, L.P., Long, Y., Hu, M., Liao, M.X., Ding, Q.L., Hu, W., Li, J.C., Hong, H., 2012. PPARgamma agonist pioglitazone reverses memory impairment and biochemical changes in a mouse model of type 2 diabetes mellitus. CNS Neurosci. Ther. 18, 659–666.
Kapogiannis, D., Boxer, A., Schwartz, J.B., Abner, E.L., Biragyn, A., Masharani, U., Frassetto, L., Petersen, R.C., Miller, B.L., Goetzl, E.J., 2015. Dysfunctionally phosphorylated type 1 insulin receptor substrate in neural-derived blood exosomes of preclinical Alzheimer's disease. FASEB J. 29, 589–596.
Kim, B., Feldman, E.L., 2012. Insulin resistance in the nervous system. Trends Endocrinol. Metab. 23, 133–141.
Kim, B., Feldman, E.L., 2015. Insulin resistance as a key link for the increased risk of cognitive impairment in the metabolic syndrome. Exp. Mol. Med. 47, e149.
Kim, J.Y., Lee, Y.W., Kim, J.H., Lee, W.T., Park, K.A., Lee, J.E., 2015. Agmatine attenuates brain edema and apoptotic cell death after traumatic brain injury. J. Korean Med. Sci. 30, 943–952.
Ko, W.C., Liu, I.M., Chung, H.H., Cheng, J.T., 2008. Activation of I(2)-imidazoline receptors may ameliorate insulin resistance in fructose-rich chow-fed rats. Neurosci. Lett. 448, 90–93.
Lee, J.H., Park, G.H., Lee, Y.K., Park, J.H., 2011. Changes in the arginine methylation of organ proteins during the development of diabetes mellitus. Diabetes Res. Clin. Pract. 94, 111–118.
Leitch, B., Shevtsova, O., Reusch, K., Bergin, D.H., Liu, P., 2011. Spatial learning-induced increase in agmatine levels at hippocampal CA1 synapses. Synapse 65, 146–153.
Liu, P., Bergin, D.H., 2009. Differential effects of i.c.v. microinfusion of agmatine on spatial working and reference memory in the rat. Neuroscience 159, 951–961.
Liu, P., Chary, S., Devaraj, R., Jing, Y., Darlington, C.L., Smith, P.F., Tucker, I.G., Zhang, H., 2008a. Effects of aging on agmatine levels in memory-associated brain structures. Hippocampus 18, 853–856.
Liu, P., Collie, N.D., Chary, S., Jing, Y., Zhang, H., 2008b. Spatial learning results in elevated agmatine levels in the rat brain. Hippocampus 18, 1094–1098.
Liu, P., Fleete, M.S., Jing, Y., Collie, N.D., Curtis, M.A., Waldvogel, H.J., Faull, R.L.,

Abraham, W.C., Zhang, H., 2014. Altered arginine metabolism in Alzheimer's disease brains. Neurobiol. Aging 35, 1992–2003.
Luo, J., Quan, J., Tsai, J., Hobensack, C.K., Sullivan, C., Hector, R., Reaven, G.M., 1998. Nongenetic mouse models of non-insulin-dependent diabetes mellitus. Metabolism 47, 663–668.
Ma, L., Wang, J., Li, Y., 2015. Insulin resistance and cognitive dysfunction. Clin. Chim. Acta 444, 18–23.
Marette, A., 2008. The AMPK signaling cascade in metabolic regulation: view from the chair. Int. J. Obes. (Lond) 32 (Suppl. 4), S3–S6.
McKay, B.E., Lado, W.E., Martin, L.J., Galic, M.A., Fournier, N.M., 2002. Learning and memory in agmatine-treated rats. Pharmacol. Biochem. Behav. 72, 551–557.
McNeilly, A.D., Williamson, R., Balfour, D.J., Stewart, C.A., Sutherland, C., 2012. A high-fat-diet-induced cognitive deficit in rats that is not prevented by improving insulin sensitivity with metformin. Diabetologia 55, 3061–3070.
McNeilly, A.D., Williamson, R., Sutherland, C., Balfour, D.J., Stewart, C.A., 2011. High fat feeding promotes simultaneous decline in insulin sensitivity and cognitive performance in a delayed matching and non-matching to position task. Behav. Brain Res. 217, 134–141.
Moore, E.M., Mander, A.G., Ames, D., Kotowicz, M.A., Carne, R.P., Brodaty, H., Woodward, M., Boundy, K., Ellis, K.A., Bush, A.I., Faux, N.G., Martins, R., Szoeke, C., Rowe, C., Watters, D.A., Investigators, A., 2013. Increased risk of cognitive impairment in patients with diabetes is associated with metformin. Diabetes Care 36, 2981–2987.
Moosavi, M., Khales, G.Y., Abbasi, L., Zarifkar, A., Rastegar, K., 2012. Agmatine protects against scopolamine-induced water maze performance impairment and hippocampal ERK and Akt inactivation. Neuropharmacology 62, 2018–2023.
Moosavi, M., Zarifkar, A.H., Farbood, Y., Dianat, M., Sarkaki, A., Ghasemi, R., 2014. Agmatine protects against intracerebroventricular streptozotocin-induced water maze memory deficit, hippocampal apoptosis and Akt/GSK3beta signaling disruption. Eur. J. Pharmacol. 736, 107–114.
Morris, R.G., Garrud, P., Rawlins, J.N., O'Keefe, J., 1982. Place navigation impaired in rats with hippocampal lesions. Nature 297, 681–683.
Morrison, C.D., Pistell, P.J., Ingram, D.K., Johnson, W.D., Liu, Y., Fernandez-Kim, S.O., White, C.L., Purpera, M.N., Uranga, R.M., Bruce-Keller, A.J., Keller, J.N., 2010. High fat diet increases hippocampal oxidative stress and cognitive impairment in aged mice: implications for decreased Nrf2 signaling. J. Neurochem. 114, 1581–1589.
Mun, C.H., Lee, W.T., Park, K.A., Lee, J.E., 2010. Regulation of endothelial nitric oxide synthase by agmatine after transient global cerebral ischemia in rat brain. Anat. Cell Biol. 43, 230–240.
Muniyappa, R., Lee, S., Chen, H., Quon, M.J., 2008. Current approaches for assessing insulin sensitivity and resistance in vivo: advantages, limitations, and appropriate usage. Am. J. Physiol. Endocrinol. Metab. 294, E15–E26.
Ozcan, U., Cao, Q., Yilmaz, E., Lee, A.H., Iwakoshi, N.N., Ozdelen, E., Tuncman, G., Gorgun, C., Glimcher, L.H., Hotamisligil, G.S., 2004. Endoplasmic reticulum stress links obesity, insulin action, and type 2 diabetes. Science 306, 457–461.
Park, Y.M., Lee, W.T., Bokara, K.K., Seo, S.K., Park, S.H., Kim, J.H., Yenari, M.A., Park, K.A., Lee, J.E., 2013. The multifaceted effects of agmatine on functional recovery after spinal cord injury through Modulations of BMP-2/4/7 expressions in neurons and glial cells. PLoS One 8, e53911.
Petrov, D., Pedros, I., Artiach, G., Sureda, F.X., Barroso, E., Pallas, M., Casadesus, G., Beas-Zarate, C., Carro, E., Ferrer, I., Vazquez-Carrera, M., Folch, J., Camins, A., 2015. High-fat diet-induced deregulation of hippocampal insulin signaling and mitochondrial homeostasis deficiences contribute to Alzheimer disease pathology in rodents. Biochim. Biophys. Acta 1852, 1687–1699.
Picone, P., Nuzzo, D., Caruana, L., Messina, E., Barera, A., Vasto, S., Di Carlo, M., 2015. Metformin increases APP expression and processing via oxidative stress, mitochondrial dysfunction and NF-kappaB activation: Use of insulin to attenuate metformin's effect. Biochim. Biophys. Acta 1853, 1046–1059.
Piletz, J.E., Aricioglu, F., Cheng, J.T., Fairbanks, C.A., Gilad, V.H., Haenisch, B., Halaris, A., Hong, S., Lee, J.E., Li, J., Liu, P., Molderings, G.J., Rodrigues, A.L., Satriano, J., Seong, G.J., Wilcox, G., Wu, N., Gilad, G.M., 2013. Agmatine: clinical applications after 100 years in translation. Drug Discov. Today 18, 880–893.
Pilon, G., Dallaire, P., Marette, A., 2004. Inhibition of inducible nitric-oxide synthase by activators of AMP-activated protein kinase: a new mechanism of action of insulin-sensitizing drugs. J. Biol. Chem. 279, 20767–20774.
Pratico, D., Uryu, K., Leight, S., Trojanoswki, J.Q., Lee, V.M., 2001. Increased lipid peroxidation precedes amyloid plaque formation in an animal model of Alzheimer amyloidosis. J. Neurosci. 21, 4183–4187.
Rahigude, A., Bhutada, P., Kaulaskar, S., Aswar, M., Otari, K., 2012. Participation of antioxidant and cholinergic system in protective effect of naringenin against type-2 diabetes-induced memory dysfunction in rats. Neuroscience 226, 62–72.
Rastegar, K., Roosta, H., Zarifkar, A., Rafati, A., Moosavi, M., 2011. The effect of Intra-CA1 agmatine microinjection on water maze learning and memory in rat. Iran. Red. Crescent Med. J. 13, 316–322.
Saltiel, A.R., Kahn, C.R., 2001. Insulin signalling and the regulation of glucose and lipid metabolism. Nature 414, 799–806.
Schubert, M., Gautam, D., Surjo, D., Ueki, K., Baudler, S., Schubert, D., Kondo, T., Alber, J., Galldiks, N., Kustermann, E., Arndt, S., Jacobs, A.H., Krone, W., Kahn, C.R., Bruning, J.C., 2004. Role for neuronal insulin resistance in neurodegenerative diseases. Proc. Natl. Acad. Sci. U. S. A. 101, 3100–3105.
Sharawy, M.H., El-Awady, M.S., Megahed, N., Gameil, N.M., 2016. Attenuation of insulin resistance in rats by agmatine: role of SREBP-1c, mTOR and GLUT-2. Naunyn Schmiedeb. Arch. Pharmacol. 389, 45–56.
Sims-Robinson, C., Kim, B., Rosko, A., Feldman, E.L., 2010. How does diabetes accelerate Alzheimer disease pathology? Nat. Rev. Neurol. 6, 551–559.
Song, J., Hur, B.E., Bokara, K.K., Yang, W., Cho, H.J., Park, K.A., Lee, W.T., Lee, K.M., Lee, J.E., 2014. Agmatine improves cognitive dysfunction and prevents cell death in a streptozotocin-induced Alzheimer rat model. Yonsei Med. J. 55, 689–699.
Stranahan, A.M., Norman, E.D., Lee, K., Cutler, R.G., Telljohann, R.S., Egan, J.M., Mattson, M.P., 2008. Diet-induced insulin resistance impairs hippocampal synaptic plasticity and cognition in middle-aged rats. Hippocampus 18, 1085–1088.
Su, C.H., Liu, I.M., Chung, H.H., Cheng, J.T., 2009. Activation of I2-imidazoline receptors by agmatine improved insulin sensitivity through two mechanisms in type-2 diabetic rats. Neurosci. Lett. 457, 125–128.
Tabak, A.G., Herder, C., Rathmann, W., Brunner, E.J., Kivimaki, M., 2012. Prediabetes: a high-risk state for diabetes development. Lancet 379, 2279–2290.
Tahara, A., Matsuyama-Yokono, A., Shibasaki, M., 2011. Effects of antidiabetic drugs in high-fat diet and streptozotocin-nicotinamide-induced type 2 diabetic mice. Eur. J. Pharmacol. 655, 108–116.
Takashima, A., 2006. GSK-3 is essential in the pathogenesis of Alzheimer's disease. J. Alzheimers Dis. 9, 309–317.
Valls-Pedret, C., Ros, E., 2013. Commentary: mediterranean diet and cognitive outcomes: epidemiological evidence suggestive, randomized trials needed. Epidemiology 24, 503–506.
Wang, C.C., Chio, C.C., Chang, C.H., Kuo, J.R., Chang, C.P., 2010. Beneficial effect of agmatine on brain apoptosis, astrogliosis, and edema after rat transient cerebral ischemia. BMC Pharmacol. 10, 11.
Watson, G.S., Peskind, E.R., Asthana, S., Purganan, K., Wait, C., Chapman, D., Schwartz, M.W., Plymate, S., Craft, S., 2003. Insulin increases CSF Abeta42 levels in normal older adults. Neurology 60, 1899–1903.
Wesson, D.W., Wilson, D.A., 2011. Age and gene overexpression interact to abolish nesting behavior in Tg2576 amyloid precursor protein (APP) mice. Behav. Brain Res. 216, 408–413.
Willette, A.A., Modanlo, N., Kapogiannis, D., Alzheimer's Disease Neuroimaging, I, 2015. Insulin resistance predicts medial temporal hypermetabolism in mild cognitive impairment conversion to Alzheimer disease. Diabetes 64, 1933–1940.
Zarifkar, A., Choopani, S., Ghasemi, R., Naghdi, N., Maghsoudi, A.H., Maghsoudi, N., Rastegar, K., Moosavi, M., 2010. Agmatine prevents LPS-induced spatial memory impairment and hippocampal apoptosis. Eur. J. Pharmacol. 634, 84–88.
Zhao, W.Q., Alkon, D.L., 2001. Role of insulin and insulin receptor in learning and memory. Mol. Cell Endocrinol. 177, 125–134.